# Engineered Stable Bioactive Per Se Amphiphilic Phosphorus Dendron Nanomicelles as a Highly Efficient Drug Delivery System To Take Down Breast Cancer In Vivo

Liang Chen, Liu Cao, Mengsi Zhan, Jin Li, Dayuan Wang, Régis Laurent, Serge Mignani, Anne-Marie Caminade, Jean-Pierre Majoral, Xiangyang Shi

# Engineered Stable Bioactive *per se* Amphiphilic Phosphorus Dendron Nanomicelles as a Highly Efficient Drug Delivery System to Take Down Breast Cancer *in Vivo*

*Liang Chen*[a,b,c#], *Liu Cao*[a#], *Mengsi Zhan*[a], *Jin Li*[a], *Dayuan Wang*[a], *Régis Laurent*[b,c], *Serge Mignani*[d,e]*, *Anne-Marie Caminade*[b,c], *Jean-Pierre Majoral*[b,c]*, *Xiangyang Shi*[a,e]*

[a] State Key Laboratory for Modification of Chemical Fibers and Polymer Materials, Shanghai Engineering Research Center of Nano-Biomaterials and Regenerative Medicine, College of Chemistry, Chemical Engineering and Biotechnology, Donghua University, Shanghai 201620, People's Republic of China

[b] Laboratoire de Chimie de Coordination du CNRS, 205 Route de Narbonne, BP 44099, 31077 Toulouse CEDEX 4, France

[c] Université de Toulouse, UPS, INPT, 31077 Toulouse CEDEX 4, France

[d] Université Paris Descartes, PRES Sorbonne Paris Cité, CNRS UMR 860, Laboratoire de Chimie et de Biochimie Pharmacologiques et Toxicologique, 45, rue des Saints Pères, 75006 Paris, France

[e] CQM - Centro de Química da Madeira, Universidade da Madeira, Campus da Penteada, 9020-105 Funchal, Portugal

**KEYWORDS:** nanomicelles; cationic phosphorus dendrons; doxorubicin; drug delivery; cancer therapy

[#] These authors contributed equally to this work.

* Corresponding author. E-mail: serge.mignani@parisdescartes.fr (S. Mignani), majoral@lcc-toulouse.fr (J. P. Majoral), and xshi@dhu.edu.cn (X. Shi)

## ABSTRACT

Conventional small molecular chemical drugs always have challenging hurdles in cancer therapy due to their high systemic toxicity and low therapeutic efficacy. Nanotechnology has been applied in drug delivery, bringing new promising potential to realize effective cancer treatment. In this context, we develop here a new nanomicellar drug delivery platform generated by amphiphilic phosphorus dendrons (1-C17G3.HCl), which could form micelles for effective encapsulation of a hydrophobic anticancer drug doxorubicin (DOX) with high drug loading content (42.4%) and encapsulation efficiency (96.7%). Owing to the unique dendritic rigid structure and surface hydrophilic groups, large steady void space of micelles can be created for drug encapsulation. The created DOX-loaded micelles with a mean diameter of 26.3 nm have good colloidal stability. Strikingly, we show that the drug-free micelles possess good intrinsic anticancer activity and enable collectively with DOX to take down breast cancer cells *in vitro* and the xenogafted tumor model *in vivo* through upregulation of Bax, PTEN, and p53 proteins for enhanced cell apoptosis. Meanwhile, the resulting 1-C17G3.HCl@DOX micelles significantly abolish the toxicity relevant to the free drug. Findings of this work demonstrate a unique nanomicelle-based drug delivery system created with the self-assembling amphiphilic phosphorus dendrons that may be adapted for chemotherapy of different cancer types.

## INTRODUCTION

Breast cancer has been considered to be the most prevailing invasive malignancy in women worldwide.[1] Although significant progresses have been achieved in early diagnosis and therapy, poor water solubility and high systemic toxicity of traditional anticancer drugs are still continuously proven to challenge the effective breast cancer therapy.[2, 3] Moreover, most drugs are quickly recognized by the mononuclear phagocyte system and consequently leading to quite a low bioavailability.[4] To address this problem, nanotechnology has been developed to create promising drug delivery systems for cancer treatment.[5-8] Nanocarrier-based drug delivery systems can overcome many bottleneck problems of conventional anticancer drugs, including high systematic toxicity and low therapeutic index, commonly associated to the instability, water insolubility, and nonspecificity of drugs.[5, 6, 8-11] Moreover, nanocarriers can be tailored to overcome multidrug resistance through improving the drug accessibility at tumor lesion *via* the known enhanced permeability and retention (EPR)-based passive tumor targeting.[12-15] Consequently, it is necessary to develop innovative nanocarrier-based systems for cancer treatment, and some of which have been in the track for clinical translation.[3, 5, 16]

Among the numerous nanoscale drug delivery systems, liposomes,[17, 18] nanogels,[19] polymer-drug conjugates,[20] dendrimers,[21] dendrons,[22] lipid-based micelles[23-25] and inorganic nanoparticles[26] have gained particular interest in nanomedicine development. The salient advantages of micelles are in two aspects: 1) high drug loading capacity to increase therapeutic potency through the improvement of the pharmacokinetic/pharmacodynamic profile of the loaded drugs; and 2) small size (< 30 nm) allowing for deep tumor penetration; 3) functionalized with specific ligands such as aptamers.[2, 24, 25, 27, 28] In general, micelles are made from amphiphilic small molecules and polymers.[2, 3, 16] Small amphiphile-based micelles have limited stability, whereas those based on amphiphilic polymers are suffering problems of dispersed molecular weight distribution.[2] Hence, an optimized nanomicelle-based delivery system is anticipated to integrate the privileges of both small and polymeric amphiphiles while overcoming their drawbacks. In line with our research in the theranostic realm, due to the biocompatibility and the numerous therapeutic applications of

phosphorus dendrimers and dendrons that have been developed by Majoral and Caminade,[29-35] we are particularly interested in the development of novel nanostructures as nanomicellar drug delivery platforms based on amphiphilic phosphorus dendrons to open new avenue in nanomedicine development. As previously reported in our group,[36] we found that cationic phosphorus dendrimers, as a kind of gene carrier, had strong gene compression and protection abilities. We also showed that core-shell tecto dendrimers with rigid cores displayed better gene compaction and delivery efficiency than the counterparts with flexible cores.[37] However, due to the strong rigidity of the phosphorous dendrimers, their hydrophobic cavity does not have drug retention ability, thus limiting their drug delivery applications. Therefore, it is crucial to design amphiphilic phosphorus dendrons, analogue of phosphorous dendrimers that can self-assemble to form micelles in aqueous solution for drug delivery applications. Previously, we designed and synthesized tyramine-bearing two dimethylphosphonate sodium salt (TBP)-modified amphiphilic phosphorus dendrons using hexachlorocyclotriphosphazene as a scaffold to modify one phosphoryl chloride group with a hydrophobic alkyl chain as a core and the other five groups to create layered phosphorous branches with P=N-P=S backbones.[38] The formed amphiphilic dendrons formed micelles in aqueous solution that were used to encapsulate hydrophobic anti-inflammatory drugs. Based on the prior study, we speculate that other amphiphilic dendrons with similar hydrophobic core and layered phosphorus branches with hydrophilic end groups may also be designed for drug delivery applications.

Here, in this original work, we report the construction and the therapeutic development of a new and effective nanomicellar platform based on generation 3 (G3) amphiphilic phosphorus dendrons for the *in vitro* and *in vivo* delivery of the anticancer drug doxorubicin (DOX), whose therapeutic efficacy has been significantly compromised by its non-specificity resulting in cumulative cardiotoxicity and nephrotoxicity.[39-41] In our work, the G3 amphiphilic phosphorus dendrons composed of rigid stable -P=N-P=S bonds were synthesized (Figure 1) from the hexachlorocyclotriphosphazene core to bear 20 hydrophobic dendritic rigid branches for hydrophobic drug encapsulation, 40 surface hydrophilic groups, and one additional hydrophobic branch of a linear alkyl chain ($C_{17}H_{35}$) for molecular self-assembly in water environment to form

micelles.[42, 43] The created micelles were used to load DOX (Figure S1) and the DOX release from the 1-C17G3.HCl@DOX micelles was investigated under different pHs. The anticancer bioactivity of the 1-C17G3.HCl@DOX micelles against MCF-7 cells (a human breast adenocarcinoma cell line) was examined *in vitro* and *in vivo* through treatment of a subcutaneous tumor model. To our knowledge, this is a very first example to create -P=N-P=S bond-containing amphiphilic phosphorous dendron-based micelles as a delivery system in cancer chemotherapy.

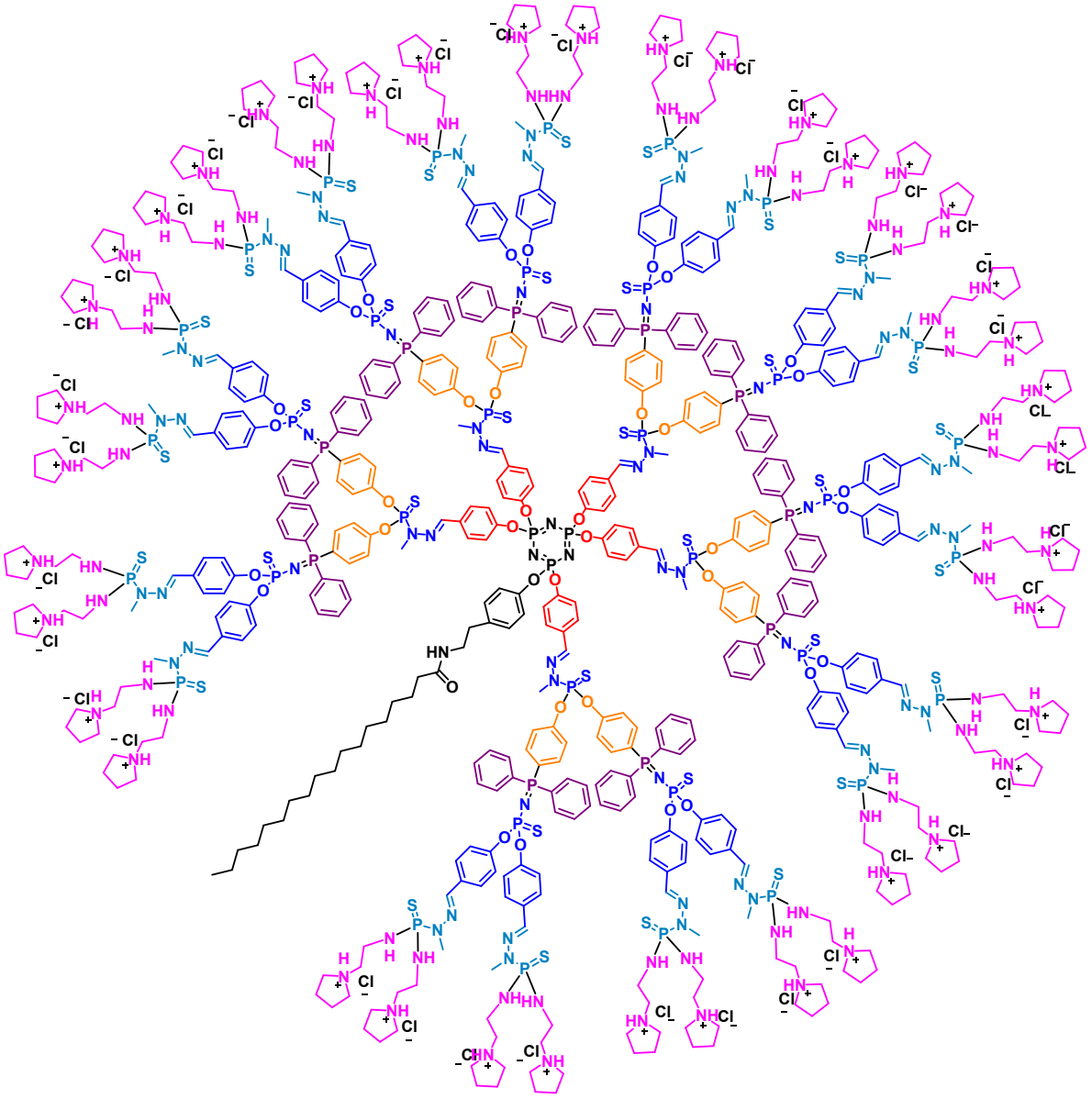

**Figure 1.** 2D chemical structure of 1-C17G3.HCl dendron.

## Experimental Section

**Synthesis of Dendron Components.** Firstly, as shown in Figure 2, the *N*-(4-hydroxyphenethyl)

stearamide (**3**) was synthesized by condensation of tyramine (**2**) with stearic acid (**1**) at room temperature in dichloromethane/methanol mixture in the presence of 1-(3-dimethylaminopropyl)-3-ethylcarbodiimide hydrochloride (EDC.HCl) as a linking agent with an 80.2% yield. The *O,O*-bis(4-formylphenyl) phosphorazidothioate (**7**) was synthesized through two steps by first condensation of 4-hydroxybenzaldehyde (**5**) with thiophosphoryl chloride (**4**) using cesium carbonate as base at room temperature in tetrahydrofuran (THF) affording (**6**) in an 80.4% yield. Nicely, under our reaction conditions, only two chlorine atoms of 4 were substituted. Condensation of sodium azide with the intermediate **6** at room temperature in THF enabled the production of compound **7** with a yield of 86.2%, which was reacted with **8** to afford the desired compound **9** with an 85.4% yield after purification. All the reaction products were analyzed by NMR (Figure S2-S11).

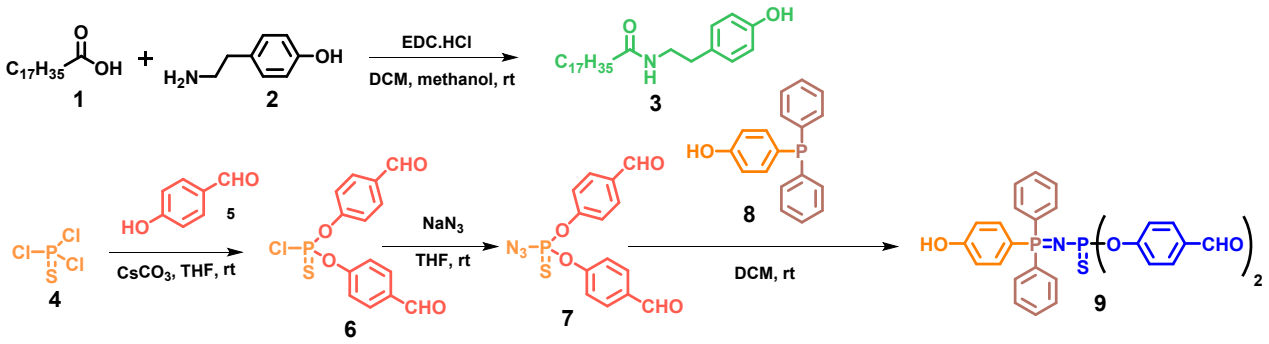


**Figure 2**. Synthesis of dendron components **3**, **7** and **9**.

**Synthesis of 1-C17G3** and **1-C17G3.HCl Dendrons.** As shown in Figure 3, the dendron 1-C17G3.HCl was obtained in seven steps from commercially available hexachlorocyclotriphosphazene (**10**). The first step is to condensate 4-hydroxybenzaldehyde (**11**) with **10** using cesium carbonate as base at room temperature leading to **12** in a 76.0% yield. Under our reaction conditions, only five chlorine atoms of **10** were substituted. The next steps are the condensation of the unique chlorine atom of **12** with **3** affording **13** with an 85.1% yield (room temperature, THF). Reaction of (1-methylhydrazineyl) phosphonothioic dichloride (**14**) with **13** in the presence of anhydrous sodium sulfate ($Na_2SO_4$) as base at room temperature in THF allows to obtain the dendron **15** (generation 1, G1) in a 90.1% yield. The next step is the increase of

generation from 1 to 2 by the reaction of **15** with **9** in THF at room temperature in the presence of anhydrous cesium carbonate ($Cs_2CO_3$) as base to afford the G2 dendron (**16**) with an 82.5% yield. Then, the condensation of **16** with **14** at room temperature in dichloromethane afforded nicely the dendron **17** in a 93.3% yield. Functionalization of the dendron **17** (generation 3) occurred by the condensation of 1-(2-aminoethyl) pyrrolidine (**18**) at room temperature in the presence of *N, N*-diisopropylethylamine as base in THF to give the dendron 1-C17G3 in a 96% yield. Finally, 1-C17G3.HCl was obtained through quantitative protonation of 1-C17G3 with HCl diethylether at room temperature in THF.

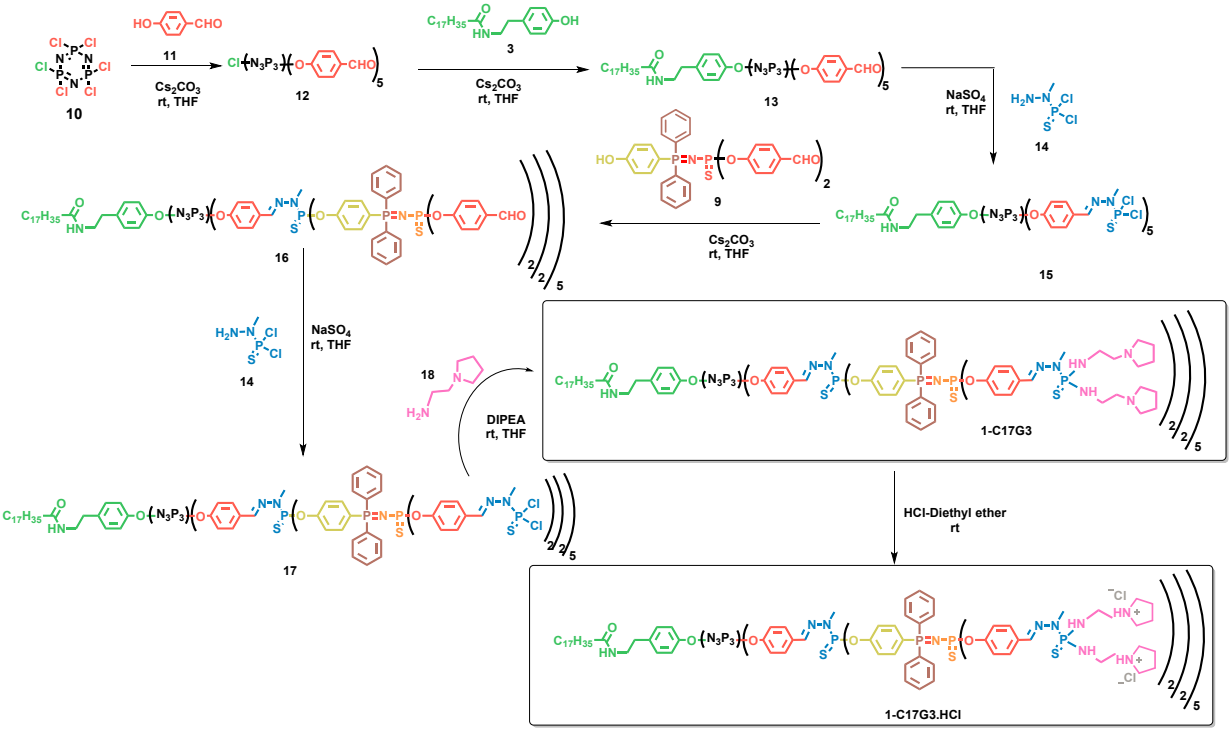


**Figure 3.** Synthesis of amphiphilic phosphorous dendrons 1-C17G3 and 1-C17G3.HCl.

**Preparation of DOX-Loaded Micelles (1-C17G3.HCl@DOX).** 1-C17G3.HCl@DOX micelles were prepared by incubating 1-C17G3.HCl and DOX under different 1-C17G3.HCl/DOX molar ratios (1: 10, 1: 15, 1: 20 or 1: 25). The mixtures were stirred overnight at room temperature and centrifuged (7000 rpm) for 20 min to take out the precipitates associated to nonencapsulated DOX. The supernatants were freeze dried for 3 days to afford the 1-C17G3.HCl@DOX complexes, which were fully characterized through transmission electron microscopy (TEM) and dynamic light

scattering (DLS) techniques.

***In Vitro* Anticancer Activity of 1-C17G3.HCl and 1-C17G3.HCl@DOX Micelles.** We tested the anticancer activity of 1-C17G3.HCl, 1-C17G3.HCl@DOX and free DOX against MCF-7 cells and normal mouse fibroblast (NIH-3T3) cells by cell counting kit-8 (CCK-8) cell viability assay. Then, cells treated with the 1-C17G3.HCl, 1-C17G3.HCl@DOX and free DOX were subjected to cellular uptake and cell apoptosis assays, the total RNA of cells were assayed by real-time quantitative polymerase chain reaction (RT-qPCR), and the cell apoptosis-related proteins were inspected *via* Western blotting.

***In Vivo* Evaluation of 1-C17G3.HCl and 1-C17G3.HCl@DOX Micelles.** All animal experiments were carried out after approval by the ethical committee for animal care of Donghua University and also in accordance with the policy of the National Ministry of Health (China). The MCF-7 xenografted tumor model was established and were intravenously injected with normal saline (NS, Group 1), 1-C17G3.HCl (Group 2), free DOX (Group 3), and 1-C17G3.HCl@DOX (Group 4), respectively on the 1$^{st}$, 4$^{th}$, 7$^{th}$ and 10$^{th}$ day. By referring to the literature,[43, 44] the dose of 5 mg DOX/kg, 7 mg 1-C17G3.HCl/kg or 12 mg 1-C17G3.HCl@DOX/kg were used for each mouse. In this case, we ensure that the used free DOX dose is effective to kill tumors but can create some side effects. The tumor volumes and the body weights were recorded every third day. After 17 days, the tumor tissues and the main organs were removed from sacrificed mice for hematoxylin & eosin staining (H&E) and TdT-mediated dUTP Nick-End Labeling (TUNEL) staining. Meanwhile, RT-qPCR and Western blot assays were also carried out to determine the apoptosis-related proteins in tumor cells in the mRNA and protein expression levels.

## RESULTS AND DISCUSSION

**Synthesis and Characterization of Amphiphilic Phosphorus Dendrons.** As revealed in Figures 1 and 2, we took advantage of the rigidity of both joined polyphenol and triphenyl-phosphanimine moieties to synthesize amphiphilic phosphorus dendrons of 1-C17G3 and 1-

C17G3.HCl bearing a linear hydrophobic alkyl chain ($C_{17}H_{35}$). These dendrons and their intermediate products were fully characterized by $^{1}H$, $^{13}C$ and $^{31}P$ NMR (Figures S2-S11, Supporting Information). Likely due to the complex structure and large molecular weight of the 1-C17G3.HCl, we were unable to determine their Mw by mass spectrometry. However, we used $^{1}H$ NMR to calculate the ratio of the methylene protons of the terminal five membered ring, protons of benzene ring, and the methylene protons of long hydrophobic alkyl chain, which is sufficient to ensure the successful structural characterization. The same problem also exists for some polyamino acids reported in the literature,[45, 46] where molar mass of the polymers could be determined using the integral ratio of the phenyl peaks and the methyl/ethyl peak of the repeating units.

**Preparation and Characterization of 1-C17G3.HCl@DOX Micelles.** Due to the amphiphilic nature of the dendron structure,[47] drug-free 1-C17G3.HCl micelles were first prepared. The critical micelle concentration (CMC) of 1-C17G3.HCl micelles was determined using a fluorescence probe method. The value of CMC was determined to be 27.0 μM (Figure 4A). As revealed by both TEM and DLS analysis, 1-C17G3.HCl micelles were successfully formed through self-assembly in water. The micelles display a spherical morphology with an average diameter of 24.5 nm (Figure 4B), and have a hydrodynamic size and zeta potential of 159.0 nm (Figure 4C) and +19.6 ± 5.0 mV (Table S1), respectively. Notably, the hydrodynamic size of the 1-C17G3.HCl micelles is very different from that measured by TEM. This discrepancy should be because TEM measures dried particles deposited onto carbon-coated copper grid, while DLS measures particles in aqueous solution that may aggregate in a certain degree.[43] Very importantly, we show that even after diluted for several times, the hydrodynamic size of the drug-free micelles has no significant change (5 μM, ~161 nm, Figure 4D). It means that the drug-free micelles formed by 1-C17G3.HCl have an excellent structural stability, which is amenable for their drug delivery applications.

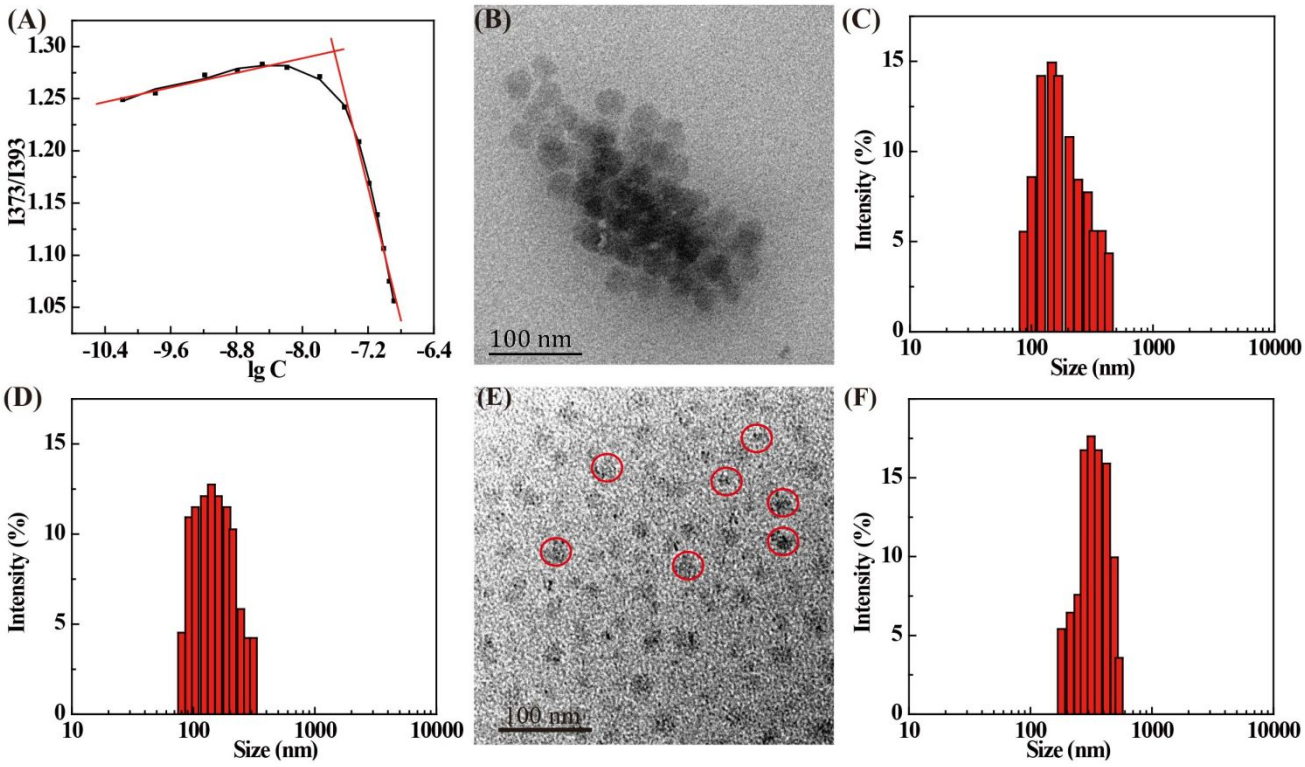


**Figure 4.** (A) The critical micelle concentration of amphiphilic phosphorous dendrons (1-C17G3.HCl) determined using the fluorescent dye pyrene. (B) TEM image and (C) DLS analysis of 1-C17G3.HCl micelles at the dendron concentration of 130.0 μM. (D) DLS analysis of 1-C17G3.HCl micelles at a concentration (5 μM) much lower than their CMC. (E) TEM image and (F) DLS analysis of 1-C17G3.HCl@DOX micelles at the dendron concentration of 76.3 μM.

We next prepared DOX-loaded micelles of 1-C17G3.HCl@DOX using the same self-assembly method.[47] By varying the dendron/DOX molar ratio, the drug loading capacity and efficiency of 1-C17G3.HCl@DOX micelles were optimized. As shown in Table S2, the maximal drug loading content is up to 42.4% with an encapsulation efficiency of 96.7% under the dendron/DOX molar ratio of 1: 20. This high drug-loading content and encapsulation efficiency of DOX can be explained by the –P=N-P=S bond-rendered molecular rigidity of the 1-C17G3.HCl micelles, leading to internal hydrophobic domains for each dendron composed of 11 benzene rings and phosphor-carbon double bonds *per* branch directly grafted on the core ring (*vide supra*). Hence, the hydrophobic drug such as DOX can be easily and stably encapsulated within the hydrophobic domain of the micelles. Meanwhile, the 1-C17G3.HCl@DOX with the 1-C17G3.HCl/DOX molar ratio at 1: 20 was selected

for subsequent studies.

The morphology and size of the 1-C17G3.HCl@DOX micelles were examined by TEM and DLS. Interestingly, the 1-C17G3.HCl@DOX micelles also exhibit a spherical shape as same as the drug-free 1-C17G3.HCl micelles, and have a mean particle size of 26.3 nm revealed by TEM (Figure 4E) and a hydrodynamic size of 277.0 nm revealed by DLS (Figure 4F). It should be noted that the small-sized nanoparticles like observed with the 1-C17G3.HCl@DOX micelles are very promising for effective anticancer drug delivery through successful escape from kidney excretion and spleen sequestration to effectively accumulate at tumor lesion with deep penetration.[25, 48, 49] Also, it is interesting to note that the 1-C17G3.HCl@DOX micelles are a little larger than the empty drug-free 1-C17G3.HCl micelles as shown with both TEM imaging and DLS analysis (Figures 4B-C and 4E-F). This discrepancy might be attributed to a micellar expansion[2] and surface potential change (Table S1) that are induced by the accommodation of DOX within the hydrophobic micellar core.

Then, the fluorescence emission and excitation spectra of free DOX and 1-C17G3.HCl@DOX micelles were investigated (Figure 5A-B). Clearly, DOX and 1-C17G3.HCl@DOX have the same fluorescence emission and excitation features. The fluorescence intensity of free DOX is approximately 2 times higher that of 1-C17G3.HCl@DOX micelles at the same equivalent DOX concentrations. In addition, as can be seen in Figure 5A-B, both free DOX and 1-C17G3.HCl@DOX show strong fluorescence intensity at a lower DOX concentration. This phenomenon can be explained by the aggregation-caused fluorescence quenching of DOX. For the 1-C17G3.HCl@DOX micelles, due to the micellar confinement effect, the encapsulated DOX molecules should have enhanced intermolecular interaction, thus having a more fluorescence quenching effect than free DOX under the same DOX concentrations.

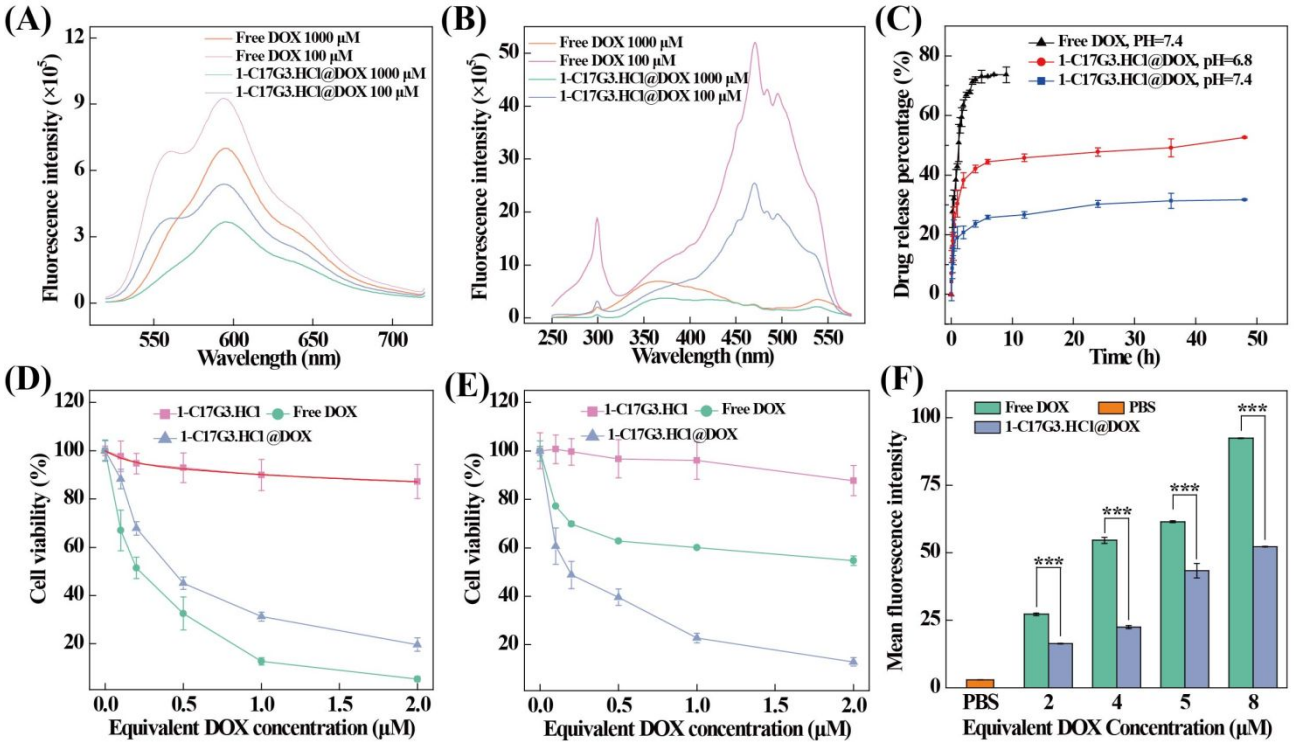


**Figure 5.** Steady-state fluorescence emission (A) and excitation (B) spectra of 1-C17G3.HCl@DOX micelles and free DOX at the DOX concentration of 100 μM and 1000 μM (excitation wavelength = 365 nm and emission wavelength = 595 nm). (C) Accumulated DOX release from 1-C17G3.HCl@DOX micelles at pH 6.8 (cytosolic pH) and pH 7.4 (physiologic pH) at 37 °C. CCK-8 assay of the viability of NIH-3T3 (D) and MCF-7 (E) cells treated with 1-C17G3.HCl, free DOX and 1-C17G3.HCl@DOX under different equivalent DOX concentrations. (F) Flow cytometry assay of the cellular uptake of free DOX and 1-C17G3.HCl@DOX micelles under different equivalent DOX concentrations.

For efficient anticancer drug delivery, it is vital for the delivery system to control the release of the therapeutic agent at the tumor site, thereby reducing its side effects to normal tissues. Since the tumor lesion is often more acidic than normal tissues, drug release at a low pH should be beneficial for cancer therapy.[50, 51] As shown in Figure 5C, the *in-vitro* DOX release from the 1-C17G3.HCl@DOX micelles ([DOX] = 1 mg/mL and [1-C17G3.HCl] = 91 μM) was examined at 37 ℃ and in phosphate buffer at pH 6.8 and pH 7.4, respectively. Approximately 46% and 27% of DOX can be released from micelles within the first 12 h at pH 6.8 and pH 7.4, respectively, followed by

continuous slow release. Additionally, the faster release of DOX at pH 6.8 than at pH 7.4 should be presumably due to the protonation of DOX under a basic condition to have an improved water solubility, thus inducing the extirpation of DOX from the micelles, in good agreement with the literature.[52]

***In Vitro* Anticancer Activity of 1-C17G3.HCl@DOX Micelles.** Since several years, we have been embarked in the development a novel nanoplatforms against tumors in general and breast cancers in particular.[22, 36, 53] Firstly, we chose the common breast adenocarcinoma (MCF-7) cells to assess the *in vitro* anticancer efficacy of 1-C17G3.HCl@DOX micelles through CCK-8 cell viability assays *versus* free DOX and *versus* normal NIH-3T3 mouse fibroblast cells for safety purpose. As can be clearly seen in Figure 5D, the cytotoxicity of free DOX against NIH-3T3 cells was 2.5 and 3.7 times higher than that of 1-C17G3.HCl@DOX at the equivalent DOX concentration of 1 and 2 μM, respectively. To be opposed, the viability of NIH-3T3 cells treated with the drug-free 1-C17G3.HCl micelles slightly decreases (12%), suggesting that the drug-free 1-C17G3.HCl micelles have a good cytocompatibility. As revealed in Figure 5E, both free DOX and 1-C17G3.HCl@DOX micelles exhibit a DOX concentration-dependent cytotoxicity against MCF-7 cells. Significantly different from the treatment of normal NIH-3T3 cells, under the same DOX concentrations, the 1-C17G3.HCl@DOX micelles show much higher cytotoxicity to MCF-7 cells than free DOX. Based on these experiments, the $IC_{50}$s of free DOX and 1-C17G3.HCl@DOX micelles were calculated to be 0.22 μM (NIH-3T3 cells)/3.28 μM (MCF-7 cells) and 0.42 μM (NIH-3T3 cells)/0.23 μM (MCF-7 cells), respectively. The safety indexes, $IC_{50}$ NIH-3T3/$IC_{50}$ MCF-7 ratios of different formulations were thus calculated to be 0.067 and 1.87 for free DOX and 1-C17G3.HCl@DOX micelles, respectively. Clearly, the 1-C17G3.HCl@DOX micelles display a much higher safety index than free DOX.

To elucidate the mechanism associated to the enhanced antiproliferation activity of 1-C17G3.HCl@DOX micelles, we first checked their uptake by MCF-7 cells using flow cytometry (Figure S12 and Figure 5F). After 4 h incubation, cells treated with both free DOX and 1-C17G3.HCl@DOX micelles display DOX concentration-dependent mean fluorescence increase,

suggesting the efficient DOX uptake in a DOX dose-dependent manner (Figure 5F). Due to the aggregation-caused fluorescence quenching of DOX, the fluorescence intensity of free DOX is approximately 2 times higher than that of 1-C17G3.HCl@DOX micelles at the same equivalent DOX concentrations (Figure 5A-B). However, the mean fluorescence intensity of free DOX-treated cells is only 1.4 times higher than that of 1-C17G3.HCl@DOX-treated cells at the same equivalent DOX concentrations (Figure 5F). Therefore, we can conclude that the 1-C17G3.HCl@DOX micelles actually have a better cellular uptake tendency.

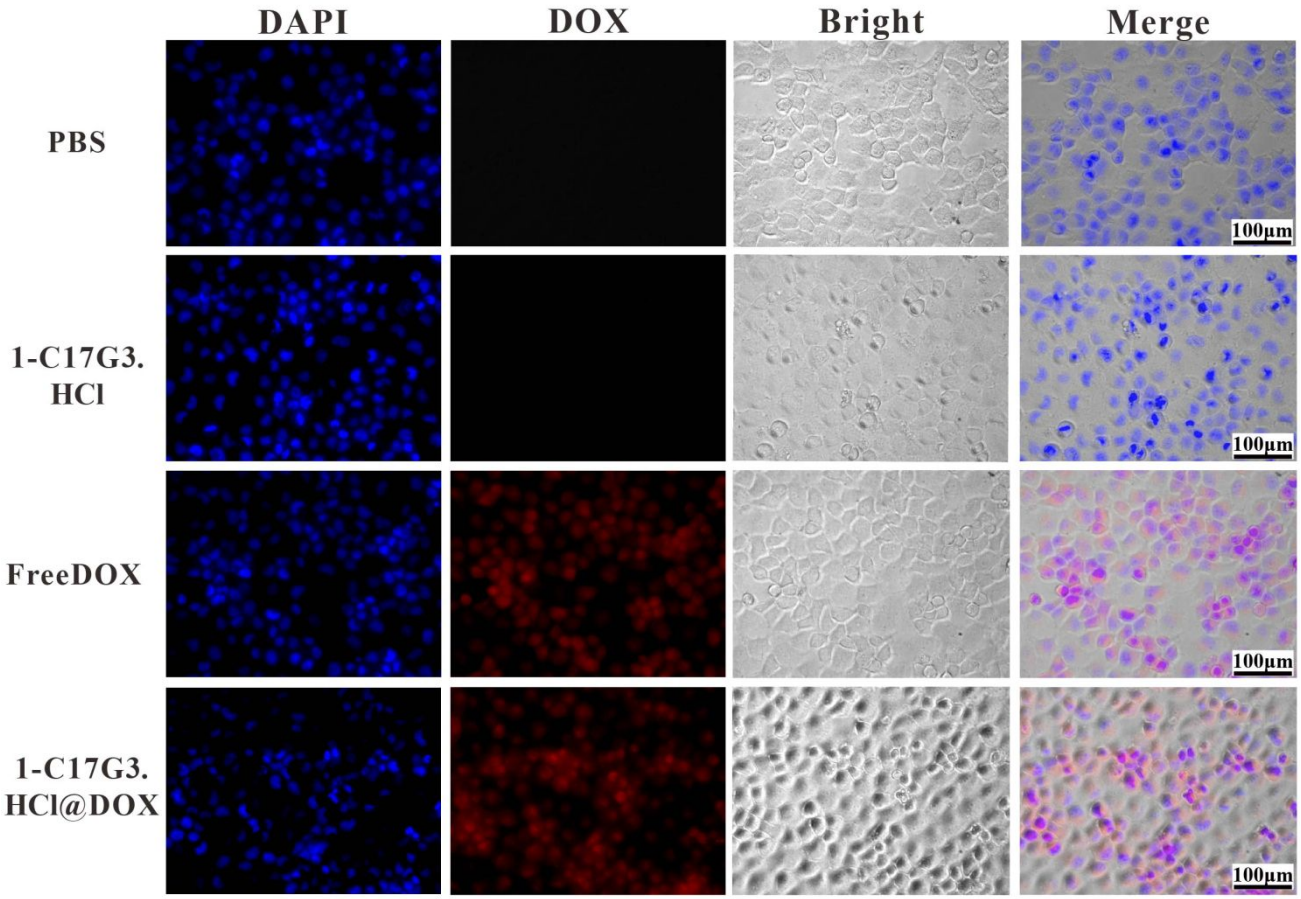


**Figure 6.** Fluorescence microscopic images of MCF-7 cells treated with PBS, 1-C17G3.HCl micelles, free DOX and 1-C17G3.HCl@DOX micelles for 5 h at an equivalent DOX concentration of 10 μM.

Furthermore, fluorescence microscopic imaging was also employed to monitor the intracellular uptake of 1-C17G3.HCl@DOX micelles (Figure 6). In the merged images, the red fluorescence was partly co-localized within the cytoplasm, indicating that both free DOX and 1-C17G3.HCl@DOX

micelles can be internalized in the cells. In sharp contrast, cells treated with PBS and DOX-free 1-C17G3.HCl micelles just show the 4', 6-diamidino-2-phenylindole (DAPI)-stained blue cell nuclei. It is interesting to note that for the group of 1-C17G3.HCl@DOX micelles, the red fluorescence signals could come from both 1-C17G3.HCl@DOX micelles and the released free DOX since more than 20% of the loaded DOX may be released after 5 h incubation with cells (Figure 5C). Taken together, these data suggest that the 1-C17G3.HCl@DOX micelles can be taken up by the MCF-7 cells possibly *via* the dominant process of phagocytosis.[54]

To investigate the promoting effect of 1-C17G3.HCl@DOX micelles on cell apoptosis, MCF-7 cells treated with free DOX and 1-C17G3.HCl@DOX micelles were assayed by flow cytometry (Figure S13 and Figure 7A). Notably, the treatment of drug-free 1-C17G3.HCl micelles obviously leads to a cell apoptosis rate of 30.19 ± 0.90%, which is much higher than that of the control group (4.22 ± 1.29%, $p < 0.001$), suggesting the inherent apoptosis-promoting effect of the drug-free 1-C17G3.HCl micelles. Meanwhile, MCF-7 cells treated with the 1-C17G3.HCl@DOX micelles have an apoptosis percentage of 66.58 ± 0.07%, which is greater than that of the drug-free 1-C17G3.HCl micelles (30.19 ± 0.90%, $p < 0.001$) and free DOX (46.08% ± 0.21%, $p < 0.001$). These results fully confirm that the developed 1-C17G3.HCl@DOX micelles taking the advantage of the bioactive *per se* drug-free 1-C17G3.HCl micelles display the best therapeutic efficacy among all groups.

To delineate the molecular mechanism associated to cell apoptosis, the relative mRNA expression of the tumor suppressor PTEN (phosphatase and tensin homologue), p53 which in turn promotes apoptosis of tumor cells and is considered to be a key indicator of antitumor drugs,[55, 56] as well as the proapoptotic protein Bax[57] were inspected using RT-qPCR (Figure 7B). MCF-7 cells treated with PBS were used as negative control. Clearly, significant increases in mRNA expression of Bax, p53 and PTEN can be nicely seen in cells treated with free DOX and 1-C17G3.HCl@DOX micelles. Meanwhile, the 1-C17G3.HCl group display slight increases in the mRNA expression of all three indicators when compared to the PBS control. RT-qPCR evaluation shows that the bioactive *per se* 1-C17G3.HCl significantly enhances the apoptosis effect of DOX (for PTEN and p53, $p < 0.01$), quite matching the results of cell apoptosis assay.

Further, the cell apoptosis-related proteins were determined using Western blotting. As shown in Figure 7C-F, significant upregulation of Bax, p53 and PTEN proteins can be observed in cells treated with drug-free 1-C17G3.HCl micelles, free DOX and 1-C17G3.HCl@DOX micelles. The expression levels of apoptosis-related proteins are the highest for the 1-C17G3.HCl@DOX group *versus* other groups ($p < 0.01$), in good agreement with the results of cell apoptosis assay and RT-qPCR. Therefore, we can conclude that the 1-C17G3.HCl micelles can be considered as a good hydrophobic drug carrier to improve the effectiveness of chemotherapy.

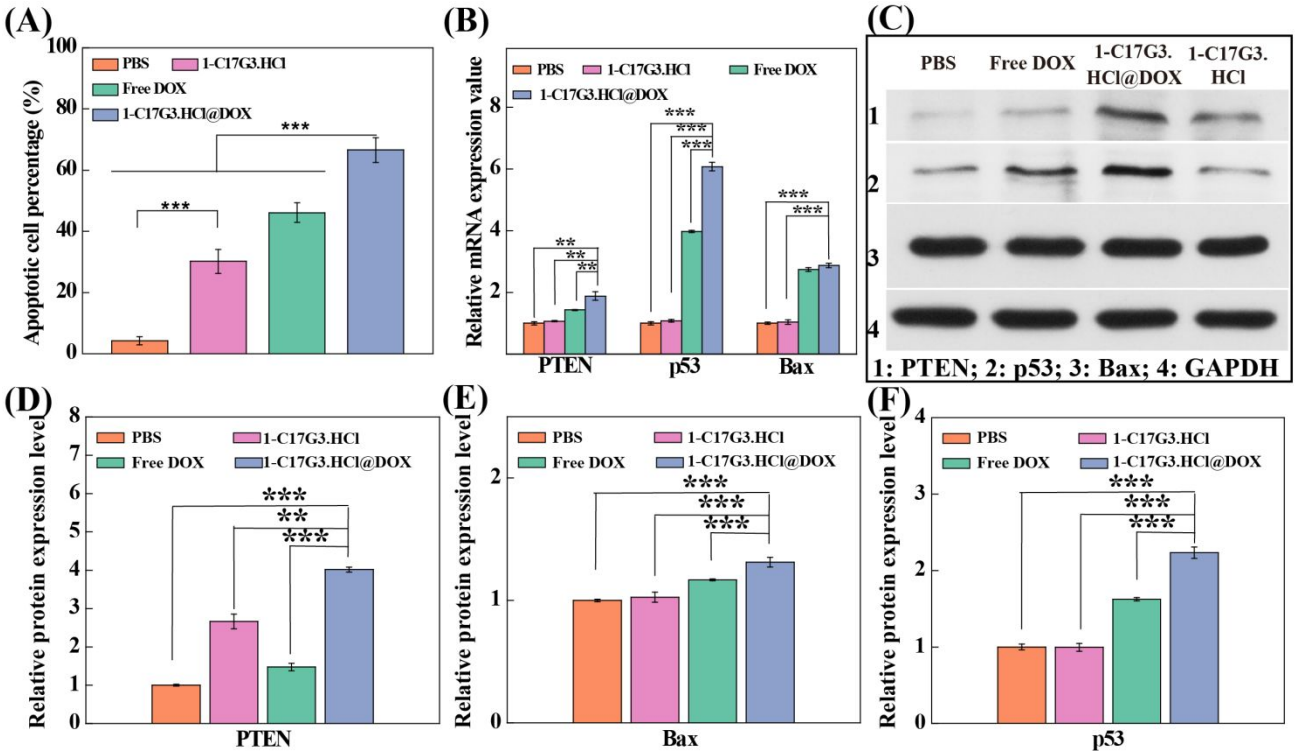


**Figure 7.** (A) Histograms of cell apoptosis percentage. (B) Validation of relative mRNA expression levels of PTEN, p53 and Bax in MCF-7 cells incubated with PBS, drug-free 1-C17G3.HCl micelles, free DOX and 1-C17G3.HCl@DOX micelles ([DOX] = 5 μM or [1-C17G3.HCl] = 0.25 μM), respectively for 24 h. (C) Western blot assay of the expression of proteins related to cell apoptosis in MCF-7 cells treated with drug-free 1-C17G3.HCl micelles and 1-C17G3.HCl@DOX micelles ([DOX] = 5 μM or [1-C17G3.HCl] = 0.25 μM). PBS and free DOX were used as controls. The GAPDH protein was used as an internal control. (D, E and F) Quantitative analysis of PTEN, Bax, and p53 proteins, respectively from the Western blot assay data *in vitro*.

***In Vivo* Breast Cancer Therapy Using 1-C17G3.HCl@DOX Micelles.** Firstly, the

hemocompatibility of 1-C17G3.HCl@DOX micelles at the DOX concentration of 0.42 μM ($IC_{50}$ value) was evaluated by hemolysis assay (Figure S14). Obviously, the 1-C17G3.HCl micelles before and after DOX loading show a good hemocompatibility with hemolysis rates lower than the threshold value of 5%. This suggests that the micelles even with a positive surface potential are still hemocompatible. In addition, the pharmacokinetics of free DOX and 1-C17G3.HCl@DOX micelles was respectively examined. As shown in Figure S15, the DOX concentration in the blood significant decreases for both free DOX and 1-C17G3.HCl@DOX groups within the first 12 h, and the 1-C17G3.HCl@DOX micelles display a much longer half-decay time (2.98 h) than free DOX (1.6 h). A subcutaneous breast tumor model was established to assess the antitumor efficacy of the developed 1-C17G3.HCl@DOX micelles in BALB/c nude mice. As shown in Figure S16 and Figure 8A, administration of free DOX and 1-C17G3.HCl@DOX micelles leads to significant tumor growth inhibition. Meanwhile, the tumor volume in the 1-C17G3.HCl group is much smaller than in the NS group, suggesting the inherent antitumor activity of the active *per se* 1-C17G3.HCl micelles. During the whole treatment period, the mice treated with NS, 1-C17G3.HCl and 1-C17G3.HCl@DOX do not show any abnormal behavior, and the mouse body weight does not show any significant loss (Figure 8B), suggesting that both 1-C17G3.HCl and 1-C17G3.HCl@DOX have no significant toxicity within experimental period. To be opposed, significant weight loss was induced in mice treated with free DOX. Furthermore, due to the high systemic toxicity of free DOX,[56, 58, 59] one mouse treated with free DOX passed away during the treatment period (Figure 8C). In contrast, in the 1-C17G3.HCl@DOX and 1-C17G3.HCl groups, all mice stay in good physical condition, similar to the NS group. This means that these micelles effectively reduce the systemic toxicity of DOX to mice.

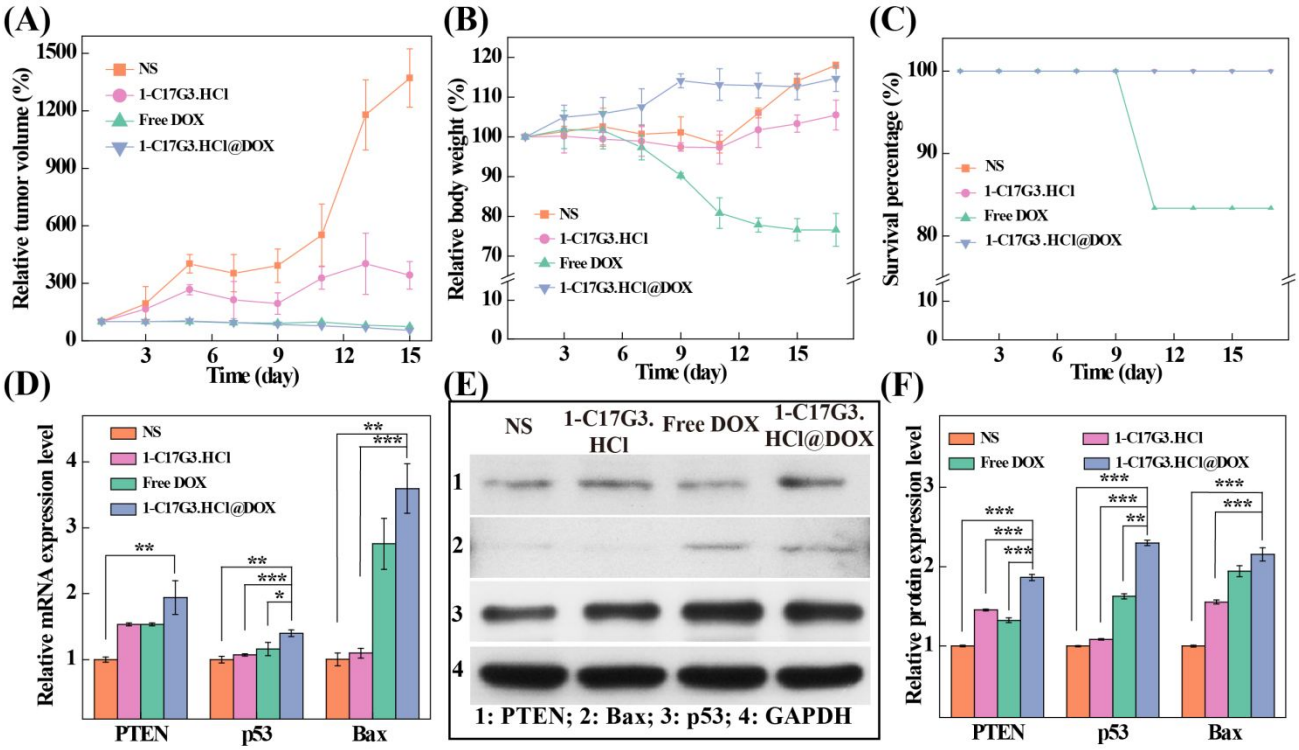


**Figure 8.** (A) Relative tumor volume at indicated time points (n = 6 for each group). (B) The relative body weights of mice at indicated time points (n = 6 for each group). (C) The survival percentages of mice at indicated time points. (D) Relative mRNA expression level of PTEN, p53 and Bax in xenografted tumor cells at 7 days post treatment of NS, 1-C17G3.HCl, free DOX and 1-C17G3.HCl@DOX (5 mg DOX/kg or 7 mg 1-C17G3.HCl/kg for each mouse). (E) Western blot assay of the PTEN, p53 and Bax proteins in xenografted tumor cells at 7 days post treatment of NS, 1-C17G3.HCl, free DOX and 1-C17G3.HCl@DOX (5 mg DOX/kg or 7 mg 1-C17G3.HCl/kg for each mouse). NS and free DOX were used as controls. The GAPDH protein was used as an internal control. (F) Quantitative analysis of PTEN, p53 and Bax proteins from the Western blot assay data *in vivo*.

After injection for 17 days, we processed the tumor tissue to isolate the tumor cells for RT-qPCR and Western blot assay of the mRNA and protein expressions (Figure 8D-F). Clearly, the tumor cells treated with the 1-C17G3.HCl@DOX micelles have the highest mRNA and protein expression levels of PTEN, p53 and Bax than all other groups, in good agreement with the *in vitro* data (Figure 7B-F). The tumor tissue samples were further subjected to histological analysis *via* H&E and TUNEL staining. As illustrated in Figure 9, the tumors treated with the 1-

C17G3.HCl@DOX micelles display the highest level of necrotic (H&E) and apoptotic (TUNEL) cell populations, indicating that the 1-C17G3.HCl@DOX micelles have the best therapeutic effect among all groups. Furthermore, quantitative assessment of the cell apoptosis rate through the TUNEL-staining images (Figure S17) reveals the cell apoptosis rate in the order of 1-C17G3.HCl@DOX (75.7 ± 4.12%) > free DOX (31.3 ± 5.40%) > 1-C17G3.HCl (13.6 ± 2.72%) > NS (4.2 ± 1.35%). This result corroborates those obtained above (Figure S13 and Figure 7A). Collectively, these results suggest that the 1-C17G3.HCl@DOX micelles exert *in vivo* anticancer effects and exhibit the most potent tumor inhibition ability.

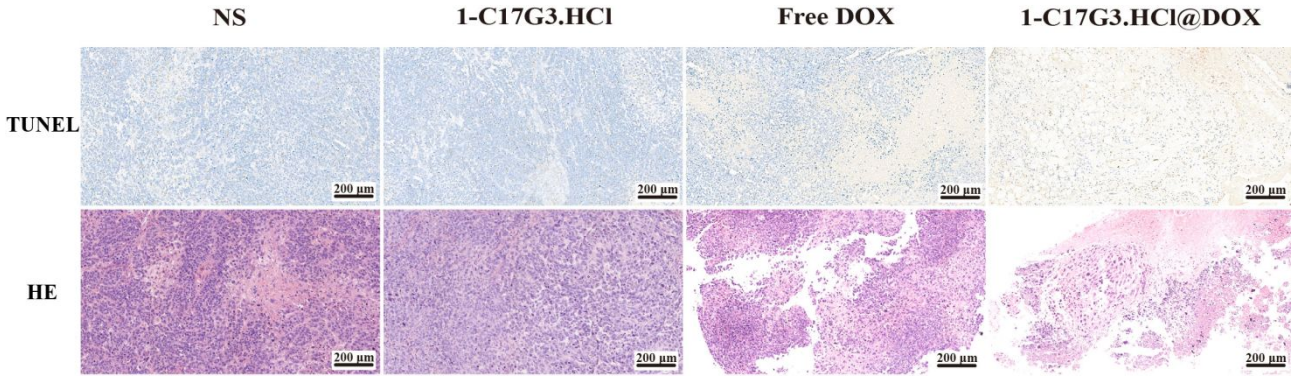


**Figure 9.** TUNEL and H&E staining of xenografted tumor sections from mice injected with NS, 1-C17G3.HCl, free DOX and 1-C17G3.HCl@DOX at 17 days post-injection. Scale bar in each panel represents 200 μm.

H&E staining was also utilized to investigate the histological features of major organs of tumor-bearing mice in different treatment groups (Figure S18). For the mice treated with free DOX, liver damage was detected. In contrast, the groups of C17G3.HCl and 1-C17G3.HCl@DOX do not show any visible organ damages. The drastically reduced toxicity of 1-C17G3.HCl@DOX micelles compared to free DOX can be likely deduced by the nanomicellar formulation of DOX, which promotes the EPR-based passive targeting of the drug to tumor site for tumor penetration and enhance chemotherapy. Collectively, these results confirm that the developed 1-C17G3.HCl@DOX micelles effectively improve the therapeutic effect of DOX while reducing its systemic toxicity.

## Conclusion

In a nutshell, we have designed and prepared the amphiphilic phosphorus dendrons of 1-C17G3.HCl, which can be self-assembled to form micelles for effective DOX encapsulation and tumor delivery. Each 1-C17G3.HCl dendron bears a long linear alkyl chain ($C_{17}H_{35}$) in core, -P=N-P=S bond-containing rigid molecular structure (56 benzene rings and 35 double bonds) in interior branches, and 40 protonated pyrrolidine groups on the surface. The created unique 1-C17G3.HCl dendrons can form micelles in water in the presence of anticancer drug DOX to form 1-C17G3.HCl@DOX micelles with a diameter of 26.3 nm and the high DOX loading content and encapsulation efficiency reaching up to 42.36% and 96.71%, respectively. Meanwhile, the 1-C17G3.HCl@DOX micelles have excellent colloidal stability, can release the DOX rapidly at an acidic tumor pH, and enable breast cancer cell apoptosis as verified by the upregulation of the indicators of PTEN, p53 and Bax in the mRNA and protein levels. With the small size and EPR-based passive targeting ability, the 1-C17G3.HCl@DOX micelles can be delivered to tumor region to exert effective tumor chemotherapy without side effects to normal organs. Most strikingly, we show that the -P=N-P=S bond-containing drug-free phosphorous dendron micelles owns the inherent anticancer bioactivity. The developed bioactive *per se* amphiphilic phosphorus dendron micelles could be a promising delivery system of different anticancer drugs to tackle different cancer types.

## Supporting Information

Full experimental details and data including zeta potentials, hydrodynamic sizes, drug loading content and drug encapsulating efficiency, safety indexes, sequences of upstream, downstream, and stem loop primers, NMR spectra, flow cytometry, *in vivo* tumor treatment evaluation, and H&E-staining images.

## Conflict of Interest

The authors declare no conflict of interest.

## Acknowledgements

Financial supports from the National Natural Science Foundation of China (81761148028 and 21911530230), the Science and Technology Commission of Shanghai Municipality (19XD1400100, 20520710300, 21490711500 and 20DZ2254900), the Shanghai Education Commission through the Shanghai Leading Talents Program, and the 111 Project (BP0719035) are gratefully acknowledged. J.P.M, S.M, A.M.C., and R.L. thank the collaborative NSFC−CNRS grant (from the France part) for financial support.

## REFERENCES

1. Kamangar, F.; Dores, G. M.; Anderson, W. F., Patterns of Cancer Incidence, Mortality, and Prevalence Across Five Continents: Defining Priorities to Reduce Cancer Disparities in Different Geographic Regions of the World. *J. Clin. Oncol.* **2006,** 24, (14), 2137-2150.

2. Wei, T.; Chen, C.; Liu, J.; Liu, C.; Posocco, P.; Liu, X.; Cheng, Q.; Huo, S.; Liang, Z.; Fermeglia, M.; Pricl, S.; Liang, X.-J.; Rocchi, P.; Peng, L., Anticancer Srug Nanomicelles Formed by Self-Assembling Amphiphilic Dendrimer to Combat Cancer Drug Resistance. *Proc. Natl. Acad. Sci. U. S. A.* **2015,** 112, (10), 2978-2983.

3. Svenson, S., Clinical Translation of Nanomedicines. *Curr. Opin. Solid State Mater. Sci.* **2012,** 16, (6), 287-294.

4. Garcia, K. P.; Zarschler, K.; Barbaro, L.; Barreto, J. A.; O'Malley, W.; Spiccia, L.; Stephan, H.; Graham, B., Zwitterionic-Coated "Stealth" Nanoparticles for Biomedical Applications: Recent Advances in Countering Biomolecular Corona Formation and Uptake by the Mononuclear Phagocyte System. *Small* **2014,** 10, (13), 2516-2529.

5. Chauhan, V. P.; Jain, R. K., Strategies for Advancing Cancer Nanomedicine. *Nat. Mater.* **2013,** 12, (11), 958-962.

6. Chow, E. K.-H.; Ho, D., Cancer Nanomedicine: From Drug Delivery to Imaging. *Sci. Transl.*

*Med.* **2013,** 5, (216), 216rv4.

7. Davis, M. E.; Chen, Z.; Shin, D. M., Nanoparticle Therapeutics: an Emerging Treatment Modality for Cancer. *Nat. Rev. Drug Discovery* **2008,** 7, (9), 771-782.

8. Peer, D.; Karp, J. M.; Hong, S.; FaroKhzad, O. C.; Margalit, R.; Langer, R., Nanocarriers as an Emerging Platform for Cancer Therapy. *Nat. Nanotechnol.* **2007,** 2, (12), 751-760.

9. Ferrari, M., Cancer Nanotechnology: Opportunities and Challenges. *Nat. Rev. Cancer* **2005,** 5, (3), 161-171.

10. Hubbell, J. A.; Chilkoti, A., Nanomaterials for Drug Delivery. *Science* **2012,** 337, (6092), 303-305.

11. Bourzac, K., Nanotechnology Carrying Drugs. *Nature* **2012,** 491, (7425), S58-S60.

12. Fang, J.; Nakamura, H.; Maeda, H., The EPR Effect: Unique Features of Tumor Blood Vessels for Ddrug Delivery, Factors Involved, and Limitations and Augmentation of the Effect. *Adv. Drug Delivery Rev.* **2011,** 63, (3), 136-151.

13. Matsumura, Y.; Maeda, H., A New Concept for Macromolecular Therapeutics in Cancer-Chemotherapy - Mechanism of Tumoritropic Accumulation of Proteins and the Antitumor Agent Smancs. *Cancer Res.* **1986,** 46, (12), 6387-6392.

14. Bertrand, N.; Wu, J.; Xu, X.; Kamaly, N.; Farokhzad, O. C., Cancer Nanotechnology: The Impact of Passive and Active Targeting in the Era of Modern Cancer Biology. *Adv. Drug Delivery Rev.* **2014,** 66, 2-25.

15. Prabhakar, U.; Maeda, H.; Jain, R. K.; Sevick-Muraca, E. M.; Zamboni, W.; Farokhzad, O. C.; Barry, S. T.; Gabizon, A.; Grodzinski, P.; Blakey, D. C., Challenges and Key Considerations of the Enhanced Permeability and Retention Effect for Nanomedicine Drug Delivery in Oncology. *Cancer Res.* **2013,** 73, (8), 2412-2417.

16. Schuetz, C. A.; Juillerat-Jeanneret, L.; Mueller, H.; Lynch, I.; Riediker, M.; NanoImpactNet, C., Therapeutic Nanoparticles in Clinics and under Clinical Evaluation. *Nanomedicine* **2013,** 8, (3), 449-467.

17. Hara, T.; Tan, Y.; Huang, L., In Vivo Gene Delivery to the Liver Using Reconstituted

Chylomicron Remnants as a Novel Nonviral Vector. *Proc. Natl. Acad. Sci. U. S. A.* **1997,** 94, (26), 14547-14552.

18. Koltover, I.; Salditt, T.; Radler, J. O.; Safinya, C. R., An Inverted Hexagonal Phase of Cationic Liposome-DNA Complexes Related to DNA Release and Delivery. *Science* **1998,** 281, (5373), 78-81.

19. Oh, J. K.; Drumright, R.; Siegwart, D. J.; Matyjaszewski, K., The Development of Microgels/Nanogels for Drug Delivery Applications. *Prog. Polym. Sci.* **2008,** 33, (4), 448-477.

20. Ekladious, I.; Colson, Y. L.; Grinstaff, M. W., Polymer-Drug Conjugate Therapeutics: Advances, Insights and Prospects. *Nat. Rev. Drug Discovery* **2019,** 18, (4), 273-294.

21. Mendes, L. P.; Pan, J.; Torchilin, V. P., Dendrimers as Nanocarriers for Nucleic Acid and Drug Delivery in Cancer Therapy. *Molecules* **2017,** 22, (9).

22. Chen, L.; Fan, Y.; Qiu, J.; Laurent, R.; Li, J.; Bignon, J.; Mignani, S.; Caminade, A.-M.; Shi, X.; Majoral, J.-P., Potent Anticancer Efficacy of First-In-Class Cu-II and Au-III Metaled Phosphorus Dendrons with Distinct Cell Death Pathways. *Chem. - Eur. J.* **2020,** 26, (26), 5903-5910.

23. Liu, X. X.; Zhou, J. H.; Yu, T. Z.; Chen, C.; Cheng, Q.; Sengupta, K.; Huang, Y. Y.; Li, H. T.; Liu, C.; Wang, Y.; Posocco, P.; Wang, M. H.; Cui, Q.; Giorgio, S.; Fermeglia, M.; Qu, F. Q.; Pricl, S.; Shi, Y. H.; Liang, Z. C.; Rocchi, P.; Rossi, J. J.; Peng, L., Adaptive Amphiphilic Dendrimer-Based Nanoassemblies as Robust and Versatile siRNA Delivery Systems. *Angew. Chem., Int. Ed.* **2014,** 53, (44), 11822-11827.

24. Cabral, H.; Matsumoto, Y.; Mizuno, K.; Chen, Q.; Murakami, M.; Kimura, M.; Terada, Y.; Kano, M. R.; Miyazono, K.; Uesaka, M.; Nishiyama, N.; Kataoka, K., Accumulation of Sub-100 nm Polymeric Micelles in Poorly Permeable Tumours Depends on Size. *Nat. Nanotechnol.* **2011,** 6, (12), 815-823.

25. Chauhan, V. P.; Stylianopoulos, T.; Martin, J. D.; Popovic, Z.; Chen, O.; Kamoun, W. S.; Bawendi, M. G.; Fukumura, D.; Jain, R. K., Normalization of Tumour Blood Vessels Improves the Delivery of Nanomedicines in a Size-Dependent Manner. *Nat. Nanotechnol.* **2012,** 7, (6), 383-388.

26. Anselmo, A. C.; Mitragotri, S., A Review of Clinical Translation of Inorganic Nanoparticles.

*AAPS J.* **2015,** 17, (5), 1041-1054.

27. Cao, W.; Zhou, J.; Wang, Y.; Zhu, L., Synthesis and In Vitro Cancer Cell Targeting of Folate-Functionalized Biodegradable Amphiphilic Dendrimer-Like Star Polymers. *Biomacromolecules* **2010,** 11, (12), 3680-3687.

28. Zhou, J.; Soontornworajit, B.; Wang, Y., A Temperature-Responsive Antibody-Like Nanostructure. *Biomacromolecules* **2010,** 11, (8), 2087-2093.

29. Solassol, J.; Crozet, C.; Perrier, V.; Leclaire, J.; Beranger, F.; Caminade, A. M.; Meunier, B.; Dormont, D.; Majoral, J. P.; Lehmann, S., Cationic Phosphorus-Containing Dendrimers Reduce Prion Replication Both in Cell Culture and in Mice Infected with Scrapie. *J. Gen. Virol.* **2004,** 85, 1791-1799.

30. Klajnert, B.; Cangiotti, M.; Calici, S.; Ionov, M.; Majoral, J. P.; Caminade, A.-M.; Cladera, J.; Bryszewska, M.; Ottaviani, M. F., Interactions Between Dendrimers and Heparin and Their Implications for the Anti-Prion Activity of Dendrimers. *New J. Chem.* **2009,** 33, (5), 1087-1093.

31. Blanzat, M.; Turrin, C. O.; Aubertin, A. M.; Couturier-Vidal, C.; Caminade, A. M.; Majoral, J. P.; Rico-Lattes, I.; Lattes, A., Dendritic Catanionic Assemblies: In Vitro Anti-HIV Activity of Phosphorus-Containing Dendrimers Bearing Gal Beta(1)cer Analogues. *Chembiochem* **2005,** 6, (12), 2207-2213.

32. Poupot, M.; Griffe, L.; Marchand, P.; Maraval, A.; Rolland, O.; Martinet, L.; L'Faqihi-Olive, F. E.; Turrin, C. O.; Caminade, A. M.; Fournie, J. J.; Majoral, J. P.; Poupot, R., Design of Phosphorylated Dendritic Architectures to Promote Human Monocyte Activation. *FASEB J.* **2006,** 20, (13), 2339-2351.

33. Rolland, O.; Griffe, L.; Poupot, M.; Maraval, A.; Ouali, A.; Coppel, Y.; Fournie, J.-J.; Bacquet, G.; Turrin, C.-O.; Caminade, A.-M.; Majoral, J.-P.; Poupot, R., Tailored Control and Optimisation of the Number of Phosphonic Acid Termini on Phosphorus-Containing Dendrimers for the Ex-Vivo Activation of Human Monocytes. *Chem. - Eur. J.* **2008,** 14, (16), 4836-4850.

34. Griffe, L.; Poupot, M.; Marchand, P.; Maraval, A.; Turrin, C.-O.; Rolland, O.; Metivier, P.; Bacquet, G.; Fournie, J.-J.; Caminade, A.-M.; Poupot, R.; Majoral, J.-P., Multiplication of Human

Natural Killer Cells by Nanosized Phosphonate-Capped Dendrimers. *Angew. Chem., Int. Ed.* **2007,** 46, (14), 2523-2526.

35. Caminade, A.-M., Phosphorus Dendrimers as Nanotools against Cancers. *Molecules* **2020,** 25, (15), 3333.

36. Chen, L.; Li, J.; Fan, Y.; Qiu, J.; Cao, L.; Laurent, R.; Mignani, S.; Caminade, A.-M.; Majoral, J.-p.; Shi, X., Revisiting Cationic Phosphorus Dendrimers as a Nonviral Vector for Optimized Gene Delivery Toward Cancer Therapy Applications. *Biomacromolecules* **2020,** 21, (6), 2502-2511.

37. Wang, D., Y,; Chen, L.; Gao, Y.; Song, C.; Ouyang, Z., J.; Li, C., S,; Mignani, S.; Majoral, J.; Shi, X., Y,; Shen, M., W,, Impact of Molecular Rigidity on the Gene Delivery Efficiency of Core–Shell Tecto Dendrimers. *J. Mater. Chem. B* **2021,** 9, (31), 6149-6154.

38. Li, J.; Chen, L.; Li, C.; Fan, Y.; Zhan, M.; Sun, H.; Mignani, S.; Majoral, J.-P.; Shen, M.; Shi, X., Phosphorus Dendron Nanomicelles as a Platform for Combination Anti-Inflammatory and Antioxidative Therapy of Acute Lung Injury. *Theranostics* **2022,** 12, (7), 3407-3419.

39. Venkatesan, N.; Punithavathi, D.; Arumugam, V., Curcumin Prevents Adriamycin Nephrotoxicity in Rats. *Br. J. Pharmacol.* **2000,** 129, (2), 231-234.

40. Benzer, F.; Kandemir, F. M.; Ozkaraca, M.; Kucukler, S.; Caglayan, C., Curcumin Ameliorates Doxorubicin-Induced Cardiotoxicity by Abrogation of Inflammation, Apoptosis, Oxidative DNA Damage, and Protein Oxidation in Rats. *J. Biochem. Mol. Toxicol.* **2018,** 32, (2), 7.

41. Yilmaz, S.; Atessahin, A.; Sahna, E.; Karahan, I.; Ozer, S., Protective Effect of Lycopene on Adriamycin-Induced Cardiotoxicity and Nephrotoxicity. *Toxicology* **2006,** 218, (2-3), 164-171.

42. Bolu, B. S.; Sanyal, R.; Sanyal, A., Drug Delivery Systems from Self-Assembly of Dendron-Polymer Conjugates. *Molecules* **2018,** 23, (7), 1570.

43. Yu, T. Z.; Liu, X. X.; Bolcato-Bellemin, A. L.; Wang, Y.; Liu, C.; Erbacher, P.; Qu, F. Q.; Rocchi, P.; Behr, J. P.; Peng, L., An Amphiphilic Dendrimer for Effective Delivery of Small Interfering RNA and Gene Silencing In Vitro and In Vivo. *Angew. Chem., Int. Ed.* **2012,** 51, (34), 8478-8484.

44. Deng, X.; Cao, M.; Zhang, J.; Hu, K.; Yin, Z.; Zhou, Z.; Xiao, X.; Yang, Y.; Sheng, W.; Wu, Y.;

Zeng, Y., Hyaluronic Acid-Chitosan Nanoparticles for Co-Delivery of MiR-34a and Doxorubicin in Therapy against Triple Negative Breast Cancer. *Biomaterials* **2014,** 35, (14), 4333-4344.

45. Jia, L.; Sun, H.; Shay, J. T.; Allgeier, A. M.; Hanton, S. D., Living Alternating Copolymerization of N-Alkylaziridines and Carbon Monoxide as a Route for Synthesis of Poly-β-peptoids. *J. Am. Chem. Soc.* **2002,** 124, (25), 7282-7283.

46. Xiao, X.; Zhou, M.; Cong, Z.; Liu, L.; Zou, J.; Ji, Z.; Cui, R.; Wu, Y.; Zhang, H.; Chen, S.; Li, M.; Liu, R., Controllable Polymerization of N-Substituted β-Alanine N-Thiocarboxyanhydrides for Convenient Synthesis of Functional Poly(β-peptoid)s. *CCS Chem.* **2022**, DOI:10.31635/ccschem.022.202201840.

47. Qiu, J.; Chen, L.; Zhan, M.; Laurent, R.; Bignon, J.; Mignani, S.; Shi, X.; Caminade, A.-M.; Majoral, J.-P., Facile Synthesis of Amphiphilic Fluorescent Phosphorus Dendron-Based Micelles as Antiproliferative Agents: First Investigations. *Bioconjugate Chem.* **2021,** 32, (2), 339-349.

48. Huang, K.; Ma, H.; Liu, J.; Huo, S.; Kumar, A.; Wei, T.; Zhang, X.; Jin, S.; Gan, Y.; Wang, P. C.; He, S.; Zhang, X.; Liang, X.-J., Size-Dependent Localization and Penetration of Ultrasmall Gold Nanoparticles in Cancer Cells, Multicellular Spheroids, and Tumors in Vivo. *ACS Nano* **2012,** 6, (5), 4483-4493.

49. Wong, C.; Stylianopoulos, T.; Cui, J.; Martin, J.; Chauhan, V. P.; Jiang, W.; Popovic, Z.; Jain, R. K.; Bawendi, M. G.; Fukumura, D., Multistage Nanoparticle Delivery System for Deep Penetration into Tumor Tissue. *Proc. Natl. Acad. Sci. U. S. A.* **2011,** 108, (6), 2426-2431.

50. Mura, S.; Nicolas, J.; Couvreur, P., Stimuli-Responsive Nanocarriers for Drug Delivery. *Nat. Mater.* **2013,** 12, (11), 991-1003.

51. Torchilin, V. P., Multifunctional, Stimuli-Sensitive Nanoparticulate Systems for Drug Delivery. *Nat. Rev. Drug Discovery* **2014,** 13, (11), 813-827.

52. Du, C. L.; Deng, D. W.; Shan, L. L.; Wan, S. N.; Cao, J.; Tian, J. M.; Achilefu, S.; Gu, Y. Q., A pH-Sensitive Doxorubicin Prodrug Based on Folate-Conjugated BSA for Tumor-Targeted Drug Delivery. *Biomaterials* **2013,** 34, (12), 3087-3097.

53. Fan, Y.; Zhang, J.; Shi, M.; Li, D.; Lu, C.; Cao, X.; Peng, C.; Mignani, S.; Majoral, J.-P.; Shi, X.,

Poly(amidoamine) Dendrimer-Coordinated Copper(II) Complexes as a Theranostic Nanoplatform for the Radiotherapy-Enhanced Magnetic Resonance Imaging and Chemotherapy of Tumors and Tumor Metastasis. *Nano Lett.* **2019,** 19, (2), 1216-1226.

54. Peng, X.; Fang, S.; Ji, B.; Li, M.; Song, J.; Qiu, L.; Tan, W., DNA Nanostructure-Programmed Cell Entry via Corner Angle-Mediated Molecular Interaction with Membrane Receptors. *Nano Lett.* **2021,** 21, (16), 6946-6951.

55. Lowe, S. W.; Bodis, S.; McClatchey, A.; Remington, L.; Ruley, H. E.; Fisher, D. E.; Housman, D. E.; Jacks, T., P53 Status and the Efficacy of Cancer-Therapy In-Vivo. *Science* **1994,** 266, (5186), 807-810.

56. Octavia, Y.; Tocchetti, C. G.; Gabrielson, K. L.; Janssens, S.; Crijns, H. J.; Moens, A. L., Doxorubicin-Induced Cardiomyopathy: From Molecular Mechanisms to Therapeutic Strategies. *J. Mol. Cell. Cardiol.* **2012,** 52, (6), 1213-1225.

57. Porter, A. G.; Janicke, R. U., Emerging Roles of Caspase-3 in Apoptosis. *Cell Death Differ.* **1999,** 6, (2), 99-104.

58. Raj, S.; Franco, V. I.; Lipshultz, S. E., Anthracycline-induced Cardiotoxicity: A Review of Pathophysiology, Diagnosis, and Treatment. *Curr. Treat. Options Cardiovasc. Med.* **2014,** 16, (6), 315-315.

59. Herman, E. H.; Elhage, A. N.; Ferrans, V. J.; Ardalan, B., Comparison of the Severity of the Chronic Cardiotoxicity Produced by Doxorubicin in Normotensive and Hypertensive Rats. *Toxicol. Appl. Pharmacol.* **1985,** 78, (2), 202-214.

TOC graphic

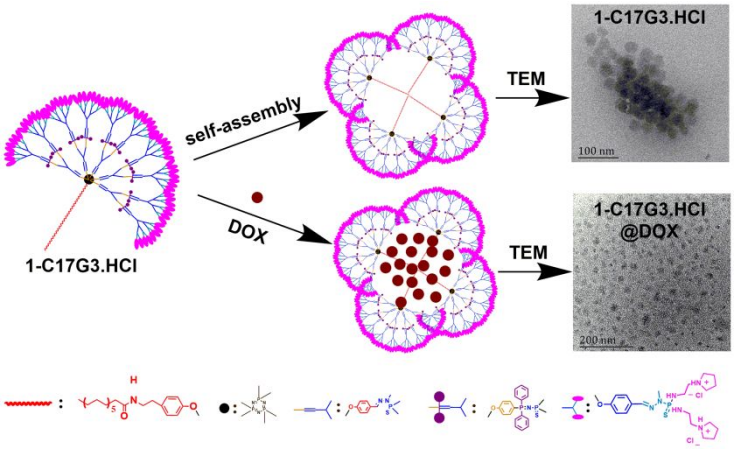
1-C17G3.HCl
self-assembly
TEM
1-C17G3.HCl
100 nm
DOX
TEM
1-C17G3.HCl
@DOX
200 nm